Intrinsic Electron Trapping in Amorphous Silicon Nitride (a-Si_3N_4:H)

Christoph Wilhelmer[1,2], Dominic Waldhoer[2], Diego Milardovich[2], Lukas Cvitkovich[2], Michael Waltl[1] and Tibor Grasser[2]
[1]Christian Doppler Laboratory for Single-Defect Spectroscopy in Semiconductor Devices at the
[2]Institute for Microelectronics, Technische Universität Wien, Gußhausstraße 27–29, 1040 Vienna, Austria
E-mail: [wilhelmer | grasser]@iue.tuwien.ac.at

***Abstract*—Silicon nitrides are widely used in electronics, most notably as the charge trapping layer of memory devices. While dangling bonds and vacancies have been identified as possible trapping centers to store charges in these materials, here we argue that intrinsic defects also contribute to the trapping and storing of electrons in amorphous Si_3N_4:H. This is because our *ab initio* investigations show that prolonged Si-N bonds can act as trapping sites for electrons in the amorphous network. The trapping sites are statistically analyzed in terms of their structural properties and bond order. By calculating relaxation energies, charge transition levels and energy barriers for charge capture and emission at these sites, we demonstrate that prolonged Si-N bonds can trap and store electrons in Si/Si_3N_4 systems, potentially contributing to the memory effect in charge trap flash devices.**

I. Introduction

Non-volatile memory devices, such as charge trap flash (CTF), use an insulating layer to store electrons, thereby reducing the leakage and increasing the number of reliable program/erase cycles compared to floating gate devices. Usually, silicon nitrides are employed as the charge storage layer of CTF, as for example realized in silicon–oxide–nitride–oxide–silicon SONOS technologies [1], due to their high trap densities ($\sim 10^{19}\,\mathrm{cm}^{-3}$ [2]). When a positive bias is applied at the gate of a CTF, electrons from the silicon channel can tunnel through the oxide layer and localize at trapping sites in the nitride layer [3], thereby changing the electrostatics and thus the threshold voltage. The nature of the defect sites responsible for the charge trapping mechanism leading to the memory effect in these devices is still unclear. Most prominently, silicon dangling bonds (K-centers) have been identified as possible amphoteric trapping centers by electronic spin resonance (ESR) measurements and theoretical calculations [4, 5]. However, the concentration of K-centers in Si_3N_4:H is rather low (10^{16}–$10^{18}\,\mathrm{cm}^{-3}$ [2, 5]), with only a fraction of them being energetically able to trap charges from a Si substrate [4]. In addition, most of the undercoordinated atoms in Si_3N_4 are passivated by H, which is present in high concentrations in this material (4-39 % H (atomic) [6]). This motivates the investigation of intrinsic trapping sites in silicon nitride, which have been suspected as possible defect centers in amorphous oxides in the recent past [4, 7].

Here, we use molecular dynamics (MD) in conjunction with a machine-learned interatomic potential (ML-IP) and density functional theory (DFT) to investigate intrinsic electron trapping in amorphous Si_3N_4:H and statistically analyze the corresponding defect parameters and structural properties. We calculate relaxation energies and charge transition levels of these sites to model the potential energy curve in two charge states and to extract energy barriers for phonon driven charge transitions.

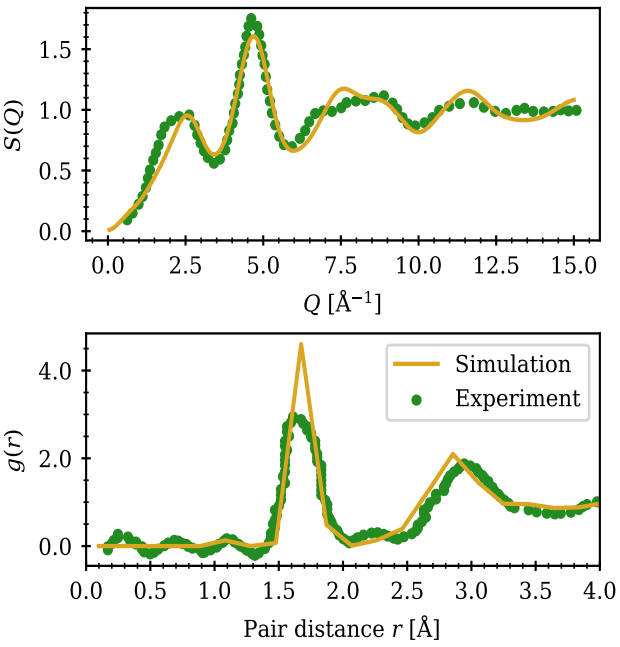

Fig. 1. Structure factor $S(Q)$ (top) and radial distribution function $g(r)$ (bottom) of our model structures compared with experimental data from Si_3N_4 thin films [8, 9].

II. Methodology

Our model Si_3N_4 structures contain 224 atoms and were created by simulating a melt-and-quench procedure using MD as implemented in the LAMMPS code [10], employing a ML-IP trained on energies, forces and stresses from single point DFT calculations of 1620 different Si_3N_4 structures to accurately model the potential energy surface (PES) of the material [11]. From the quenched structures, 11 were picked for further investigations. These structures contain less than 3% under- and overcoordinated atoms and their dangling bonds were passivated with H, resulting in a total H concentration

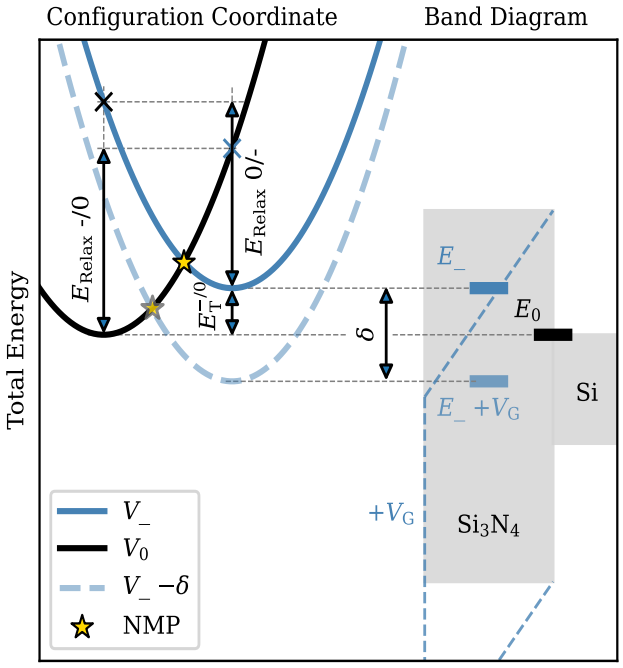

Fig. 2. Schematics of the potential energy curves (PECs) in the harmonic approximation of an electron trap in two charge states within the context of an Si/Si_3N_4 band diagram. The nonradiative charge transitions are phonon driven and occur over the crossing point NMP. An applied positive bias shifts the trap level by δ due to the electric field in the nitride.

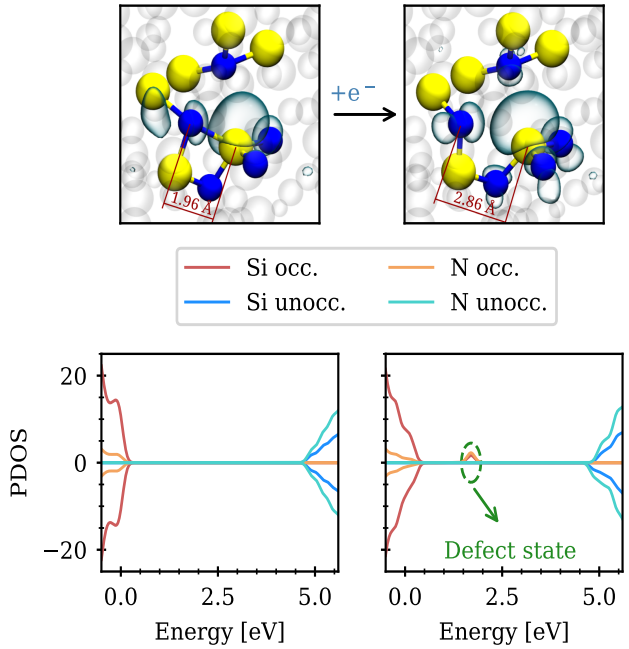

Fig. 3. Top: LUMO of neutral a-Si_3N_4:H (left) and HOMO of the negatively charged Si_3N_4:H after trapping an electron (right). Bottom: PDOS of neutral (left) and negatively charged a-Si_3N_4 with an occupied defect state in the band gap (right). Positive and negative PDOS values correspond to spin states up and down, respectively.

of $\sim 10^{22}\,\mathrm{cm}^{-3}$, which is in good agreement with the H concentration experimentally found in Si_3N_4 thin films [6, 12]. Subsequently, the quenched and passivated structures were cell relaxed with the pseudo-potential PBE and furthermore geometry optimized with a range-separated variant of the PBE0 hybrid functional [13] in charge states $q = 0$ and -1 with DFT as implemented in the CP2K code [14]. For all DFT calculations, we employed a double-ζ Gaussian basis set [15] combined with the Goedecker-Teter-Hutter (GTH) pseudopotentials [16] and an energy cutoff of $800\,\mathrm{Ry}$, using a convergence criterion for the self-consistent calculations of at least $8\,\mu$eV.

The resulting model structures have no N-N or Si-Si bonds and accurately resemble experimental structural properties of Si_3N_4 thin films such as structure factor and radial distribution function [8, 9], as shown in Fig. 1. The mass densities of the model structures are $2.97 \pm 0.03\,\mathrm{g\,cm}^{-3}$, matching the N depositing technique dependent experimental mass density values of a-Si_3N_4 ranging from 2.6 to $3.0\,\mathrm{g\,cm}^{-3}$ [17]. The band gaps of our structures are $4.66 \pm 0.23\,\mathrm{eV}$, which is in the range of experimental values from 4.5 to 5.3 eV [2]. The charge exchange process can be described by a nonradiative multi-phonon model (NMP), where the charge transfer is characterized by a phonon driven transition over the crossing point of the PECs of the system in two charge states, here denoted as the transition level NMP in Fig. 2. Hereby, electrons are exchanged with the conduction band minimum (CBM) of the Si substrate, which acts as an electron reservoir. By applying a positive gate voltage V_{G}, the defect level is changed by a level shift δ due to the occurring electric field in the oxide. Thus, δ also depends on the distance of the defect from the gate of e.g. a SONOS device. A full band diagram of a SONOS device under applied bias is for example presented in [3].

III. Results

We find that when an electron is introduced to the system, it localizes around a Si in a strained environment of the Si_3N_4:H amorphous network, thereby stretching the bond to an adjacent N by $0.57 \pm 0.25\,\text{Å}$ on average, as shown in Fig. 3 (top). The corresponding state at the CBM of the projected density of states (PDOS) is now occupied and shifts far into the a-Si_3N_4 band gap due to atomic relaxation as shown in Fig. 3 (bottom). The combined Si-N bond length distribution of all neutral structures is plotted in Fig. 5 (a), with the vertical lines corresponding to the bond getting stretched after electron capture at an adjacent Si of each structure, showing that electrons preferentially get trapped near already prolonged Si-N bonds. Due to the stretched bonds, which were also found in previous theoretical investigations [18], the bond length distribution is asymmetric, which can be accounted for by a Weibull fit in the form of

$$f(x) = \frac{b}{a}\left(-\frac{x-c}{a}\right)^{b-1} \mathrm{e}^{-\left(-\frac{x-c}{a}\right)^{b}} \qquad (1)$$

with the scale parameter a, the shape parameter b and the location parameter c. The fitting parameters for all Si-N bonds are given in the plot. Additionally, the stretched bonds were fitted with a normal distribution with the parameters given

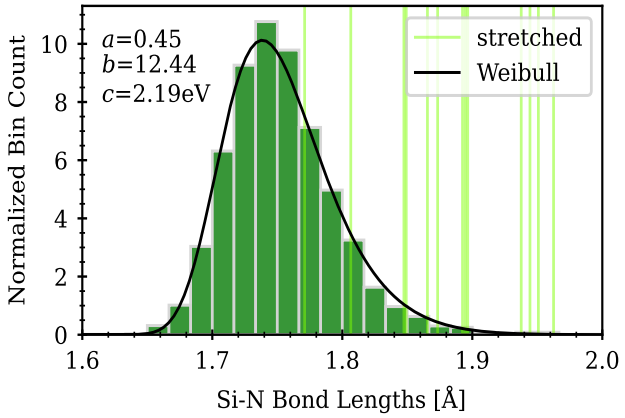

Fig. 4. Si-N bond distribution of neutral a-Si_3N_4:H with a fitted Weibull distribution (Eq. (1)) and parameters given in the plot. The stretched bonds, that break after trapping an electron, are shown as vertical lines with fitting parameters of a normal distribution given in Table I.

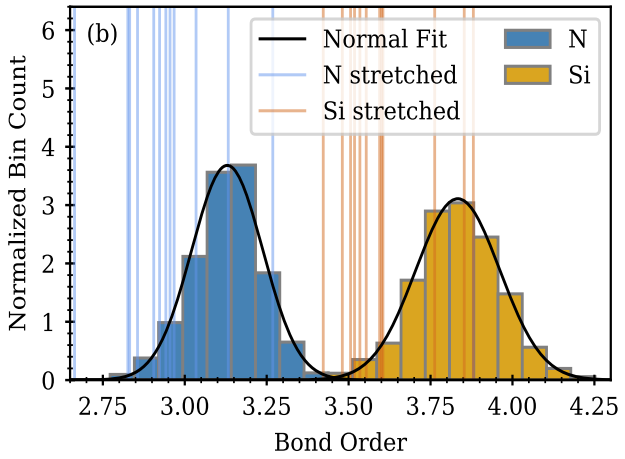

Fig. 5. Bond order distribution of neutral a-Si_3N_4:H of the 11 structures combined with the bond order of Si and N of the stretched bonds of each structure, that break after trapping an electron, shown as vertical lines. Fitting parameters are given in Table I.

in Table I. Furthermore, the distribution of the bond order (BO), which was calculated from the valence electron density with the DDEC6 method as implemented in [19], is plotted in Fig. 5 (b). The vertical lines denote the BO of the Si and N of the bond getting stretched, showing that the atoms of the trapping site are already comparably weakly bonded. Fitting parameters of normal distributions are given in Table I.

TABLE I
FITTING PARAMETERS OF NORMAL DISTRIBUTIONS FOR RELAXATION ENERGIES, BOND ORDERS AND STRETCHED BOND LENGTHS.

Normal Distribution		
Parameter	μ [eV]	σ [eV]
E_{Relax} -/0	1.55	0.27
E_{Relax} 0/-	1.39	0.28
Bond order N	3.13	0.11
Bond order N stretched	2.94	0.15
Bond order Si	3.83	0.13
Bond order Si stretched	3.61	0.14
Si-N Bond length stretched	1.88	0.05

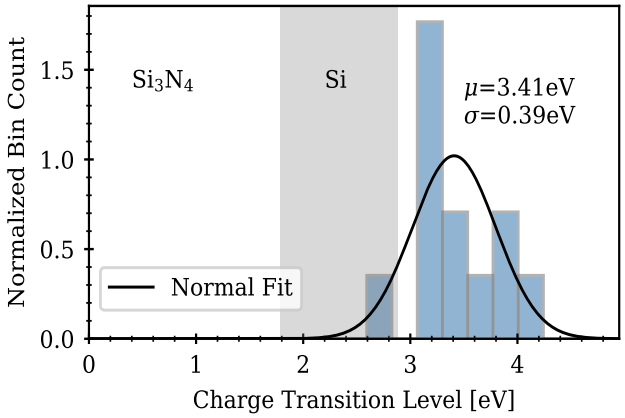

Fig. 6. Charge transition levels of intrinsic electron trapping sites in the context of a Si/Si_3N_4 band diagram with fitting parameters of a normal distribution given in the plot.

The charge transition levels (CTLs) of these sites, which correspond to the energy of the exchanged electron where the formation energies of the neutral and negatively charged systems are equal as described in [20], are shown in Fig. 6 within the context of a Si/Si_3N_4 band diagram using a Si/Si_3N_4 valence band offset of 1.78 eV from [21]. The parameters of the fitted normal distribution are given in the plot. The CTLs are distributed slighlty above the CBM of a Si substrate, showing that intrinsic sites in a-Si_3N_4 can easily trap electrons (e.g. in SONOS devices), as an applied gate bias shifts the CTL distribution to lower energies as shown in Fig. 2. Furthermore, relaxation energies E_{Relax} were calculated with DFT to model the curvature and relative position of the PECs in two charge states and were fitted with a normal distribution with the fitting parameters given in Table I. E_{Relax} also corresponds to the energy dissipated to the surrounding thermal bath following a radiative charge transition. The relaxation energies are relatively small compared to point defects in SiO_2 [20, 22], suggesting that these traps can facilitate trap-assisted tunneling and thus might not only be relevant for storing charge but also for the dynamics of charge relaxation in the trapping layer of a CTF [23].

CTLs and E_{Relax} were used to model the PEC of the 11 a-Si_3N_4:H structures in two charge states to extract the energy barriers from minimum energy configurations to the crossing point NMP of the two PECs, as shown in Fig. 2. The energy barriers for electron capture and electron emission from and to the CBM of a Si substrate are shown as a correlation plot in logarithmic scale for three different δ in Fig. 7. Initially, NMP energy barriers for electron capture are comparably high, due to the CTLs being energetically above the CBM of the Si substrate. When the trap levels are shifted to lower values by δ according to an applied positive voltage, barriers for electron capture decrease, while NMP energy barriers for electron emission are increasing. The results show, that under an applied positive voltage, the intrinsic electron trapping sites can capture and store electrons from a Si substrate.

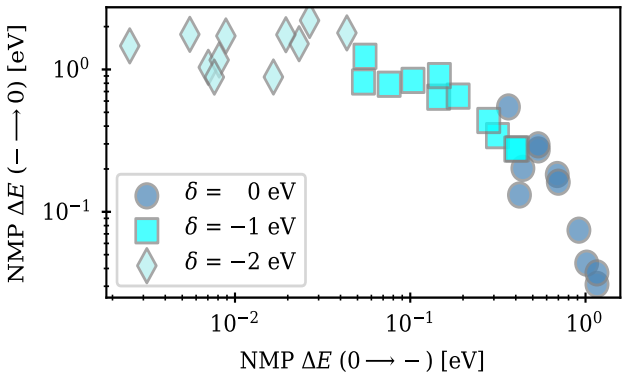

Fig. 7. Energy barriers in logarithmic scale for nonradiative multi-phonon charge transitions at intrinsic electron trapping sites in a-Si_3N_4:H, shown as a correlation plot for electron emission vs. electron capture. Barriers are given for three different trap level shifts δ generated by an applied positive gate voltage as depicted in Fig. 2.

IV. Conclusion

We analyzed the electron trapping behavior of intrinsic trapping sites in amorphous silicon nitride (a-Si_3N_4:H) using *ab initio* methods. We find that electrons can localize around weakly bonded Si, thereby further stretching an already prolonged Si-N bond, which introduces an occupied defect state in the band gap. Charge transition levels and relaxation energies of these electron traps are statistically analyzed to model the potential energy curves of the system in two charge states to extract energy barriers for electron exchange with a Si substrate. Our investigations show, that intrinsic sites in a-Si_3N_4 are able to capture and store electrons from Si substrates under an applied positive gate bias, for example during program conditions of charge trap flash, and thus can contribute to the memory effect of these devices.

Acknowledgment

The financial support by the Austrian Federal Ministry for Digital and Economic Affairs, the National Foundation for Research, Technology and Development and the Christian Doppler Research Association is gratefully acknowledged. This project was also funded by the European Union's Horizon 2020 research and innovation program under grant agreement No. 871813, within the framework of the project Modeling Unconventional Nanoscaled DeviceFABrication (MUNDFAB). Furthermore, the support from the Vienna Scientific Cluster for providing resources on the Austrian high-performance clusters VSC4 and VSC5 is gratefully acknowledged.

References

[1] J. U. Lee, K. S. Roh, G. C. Kang, S. H. Seo, K. Y. Kim, S. Lee, K. J. Song, *et al.*, "Optical capacitance-voltage characterization of charge traps in the trapping nitride layer of charge trapped flash memory devices," *Appl. Phys. Lett.*, vol. 91, 11 2007.

[2] V. A. Gritsenko, *Silicon Nitride on Si: Electronic Structure for Flash Memory Devices*, ch. 6. 2016.

[3] D.-H. Kim, S. Cho, D. H. Li, J.-G. Yun, J. H. Lee, B.-G. Park, *et al.*, "Program/erase model of nitride-based nand-type charge trap flash memories," *Jpn. J. Appl. Phys.*, vol. 49, p. 084301, Aug 2010.

[4] R. P. Vedula, S. Palit, M. A. Alam, and A. Strachan, "Role of atomic variability in dielectric charging: A first-principles-based multiscale modeling study," *Phys. Rev. B*, vol. 88, p. 205204, Nov 2013.

[5] W. L. Warren, J. Kanicki, J. Robertson, E. H. Poindexter, and P. J. McWhorter, "Electron paramagnetic resonance investigation of charge trapping centers in amorphous silicon nitride films," *J. Appl. Phys.*, vol. 74, no. 6, pp. 4034–4046, 1993.

[6] R. Chow, W. A. Lanford, W. Ke-Ming, and R. S. Rosler, "Hydrogen content of a variety of plasma-deposited silicon nitrides," *J. Appl. Phys.*, vol. 53, no. 8, pp. 5630–5633, 1982.

[7] A.-M. El-Sayed, M. B. Watkins, V. V. Afanas'ev, and A. L. Shluger, "Nature of intrinsic and extrinsic electron trapping in SiO_2," *Phys. Rev. B*, vol. 89, p. 125201, Mar 2014.

[8] M. Misawa, T. Fukunaga, K. Niihara, T. Hirai, and K. Suzuki, "Structure characterization of CVD amorphous Si_3N_4 by pulsed neutron total scattering," *J. Non-Cryst. Solids*, vol. 34, no. 3, pp. 313–321, 1979.

[9] T. Aiyama, T. Fukunaga, K. Niihara, T. Hirai, and K. Suzuki, "An X-ray diffraction study of the amorphous structure of chemically vapor-deposited silicon nitride," *J. Non-Cryst. Solids*, vol. 33, no. 2, pp. 131–139, 1979.

[10] A. P. Thompson, H. M. Aktulga, R. Berger, D. S. Bolintineanu, W. M. Brown, P. S. Crozier, *et al.*, "LAMMPS - a flexible simulation tool for particle-based materials modeling at the atomic, meso, and continuum scales," *Comp. Phys. Comm.*, vol. 271, p. 108171, 2022.

[11] D. Milardovich, C. Wilhelmer, D. Waldhoer, L. Cvitkovich, G. Sivaraman, and T. Grasser, "Machine learning interatomic potential for silicon-nitride (Si_3N_4) by active learning," *J. Chem. Phys.*, vol. 158, 05 2023. 194802.

[12] S. King, R. Chu, G. Xu, and J. Huening, "Intrinsic stress effect on fracture toughness of plasma enhanced chemical vapor deposited SiN_x:H films," *Thin Solid Films*, vol. 518, no. 17, pp. 4898–4907, 2010.

[13] M. Guidon, J. Hutter, and J. VandeVondele, "Robust periodic Hartree-Fock exchange for large-scale simulations using gaussian basis sets," *J. Chem. Theory Comput*, vol. 5, no. 11, pp. 3010–3021, 2009.

[14] T. D. Kühne, M. Iannuzzi, M. Del Ben, V. V. Rybkin, P. Seewald, F. Stein, *et al.*, "CP2K: An electronic structure and molecular dynamics software package - Quickstep: Efficient and accurate electronic structure calculations," *J. Chem. Phys.*, vol. 152, no. 19, p. 194103, 2020.

[15] J. VandeVondele and J. Hutter, "Gaussian basis sets for accurate calculations on molecular systems in gas and condensed phases," *J. Chem. Phys.*, vol. 127, no. 11, p. 114105, 2007.

[16] S. Goedecker, M. Teter, and J. Hutter, "Separable dual-space Gaussian pseudopotentials," *Phys. Rev. B*, vol. 54, pp. 1703–1710, Jul 1996.

[17] A. E. Kaloyeros, Y. Pan, J. Goff, and B. Arkles, "Review—silicon nitride and silicon nitride-rich thin film technologies: State-of-the-art processing technologies, properties, and applications," *ECS J. Solid State Sci.*, vol. 9, p. 063006, aug 2020.

[18] L. E. Hintzsche, C. M. Fang, T. Watts, M. Marsman, G. Jordan, M. W. P. E. Lamers, A. W. Weeber, and G. Kresse, "Density functional theory study of the structural and electronic properties of amorphous silicon nitrides: Si_3N_{4-x}:H," *Phys. Rev. B*, vol. 86, p. 235204, Dec 2012.

[19] T. Manz, "Introducing DDEC6 atomic population analysis: Part 3. Comprehensive method to compute bond orders," *RSC Adv.*, vol. 7, pp. 45552–45581, 09 2017.

[20] C. Wilhelmer, D. Waldhoer, M. Jech, A.-M. B. El-Sayed, L. Cvitkovich, M. Waltl, and T. Grasser, "Ab initio investigations in amorphous silicon dioxide: Proposing a multi-state defect model for electron and hole capture," *Microelectron. Reliab.*, vol. 139, no. 114801, 2022.

[21] J. W. Keister, J. E. Rowe, J. J. Kolodziej, H. Niimi, T. E. Madey, and G. Lucovsky, "Band offsets for ultrathin SiO_2 and Si_3N_4 films on Si(111) and Si(100) from photoemission spectroscopy," *J. Vac. Sci.*, vol. 17, no. 4, pp. 1831–1835, 1999.

[22] C. Wilhelmer, M. Jech, D. Waldhör, A.-M. El-Sayed, L. Cvitkovich, and T. Grasser, "Statistical Ab Initio Analysis of Electron Trapping Oxide Defects in the Si/SiO_2 Network," in *Proceedings of the European Solid-State Device Research Conference (ESSDERC)*, pp. 243–246, 2021.

[23] C. Schleich, D. Waldhör, A.-M. El-Sayed, K. Tselios, B. Kaczer, M. Waltl, *et al.*, "Single- versus multi-step trap assisted tunneling currents—Part II: The role of polarons," *Trans. Electron. Devices*, vol. 69, no. 8, pp. 4486–4493, 2022.